Journal of Corrosion and Materials
www.corromat.com

J. Corros. Mater. (2022) 1(2), 107–122.

Spectral Noise Filtering and Mean-Field Thresholds in Fractional Corrosion Reaction–Diffusion Dynamics

Peter Behrens[1,*]

[1] *Institute of Inorganic Chemistry, Leibniz University Hannover, 30167 Hannover, Germany*

*Corresponding author: peter.behrens@acb.uni-hannover.de

(Received: 15 August 2022. Received in revised form: 2 November 2022. Accepted: 28 November 2022. Published online: 30 December 2022.)

Abstract

Corrosion that varies from place to place is frequently initiated by perturbations which are not acting directly on the spatial average of the surface, coating, pore structure, or reinforcing interface but which are able to shift the spatial average of a field through nonlinear response. Here, we develop a closed fractional stochastic reaction-diffusion framework for that process. We define a normalized corrosion-activity field on $[0, \pi]$, with Neumann boundary conditions, where fractional transport is represented by the operator $(-\Delta)^{r/2}$, for $1 < r \leq 2$, and environmental variability is accounted for by finite-dimensional Wiener forcing on the stable modes of cosine functions. The critical quantity is the mean, whereas the forced high-frequency modes quickly relax due to strong diffusion. The effect of averaging the stationary fluctuations of the stable modes is the spectral weighting of their variance $\mathcal{S}_r = \sum_{j \in \mathcal{J}} \alpha_j^2/(2Dj^r)$, which plays the role of deterministic modification of the reaction law. With the case of cubic passivation and activation kinetics, the passive state is stable if $\mathcal{S}_r > 1/3$. In logistic damage growth kinetics with carrying capacity K, nonzero sustained steady-states appear exclusively if $\mathcal{S}_r \leq K^2/4$. The analysis relies on $r \in \{1.2, 1.6, 2.0\}$, one forced mode $q \in \{1, 2, 3, 4, 5\}$, $D \in \{0.5, 1.0, 1.5, 2.0\}$, and $K = 1$, except if indicated. Our findings suggest that modal positioning is as important as the amplitude, since lower frequency modes have larger leverage on the mean-field due to weak fractional diffusion damping relative to higher frequency modes. This model therefore provides a clear cut-off value for the interpretation of corrosion pattern resulting from variations in chlorides, defects in coatings, porosity, and wet-dry cycling.

Keywords: corrosion activity; stochastic reaction–diffusion; fractional Laplacian; chloride heterogeneity; spectral averaging; passivation threshold.

1. Introduction

Corrosion is seldom a uniform process converting exposed metal into corrosion products. Even a specimen of homogeneous alloy, under a seemingly uniform exposure to the surrounding environment, may exhibit damage localized to inclusions, passive film defects, coating pores, high-chloride regions, crevices, heat-affected zones, and pathways of preferential wetting. Classical corrosion engineering literature draws a distinction between general and localized corrosion phenomena such as pitting, crevice, and galvanic corrosion [1]. General corrosion modeling relates the morphology of corrosion processes to section loss and cracking in addition to lifetime estimation [2]. Corrosion-control literature highlights that the localized damage process is more important than section loss for making the decision about inspection and maintenance procedures [3]. Interfacial and surface chemistry literature also emphasizes that passive film defects and chemistry at the interface determine the location of degradation processes [4]. The mathematical problem is that different degradation histories occur from the same average chemical exposure when it varies in its spatial pattern. Mean rate corrosion law describes the total loss but not the reasons for changing the onset of persistent activity in case of spatially non-uniform exposure of zero mean.

Electrochemical approach provides a starting point in the description of charge transfer, electrochemical kinetics, and reaction rates [5]. Theory of electrochemical systems develops the description to include ionic transport and coupled migration-diffusion processes [6]. Surface chemistry approaches establish connections between these processes and passive film formation and breakdown [7]. These descriptions are mechanistically rich but hard to apply for the identification of threshold variables from incomplete spatial information. The need for threshold description becomes apparent in the case of localized corrosion. Critical review of pitting corrosion theory demonstrates that passive film breakdown alone is not sufficient for ensuring pit persistence [8]. More recent developments distinguish between the initiation and the conditions necessary for persistence and propagation of pits [9]. Pitting corrosion theory also includes the emphasis on transport limitations, local chemistry, and geometry of an active cavity preventing repassivation [10]. Recently developed theoretical framework of pitting corrosion is also concerned with the role of interfacial and transport effects in localized corrosion [11]. Reinforced concrete systems are another area where the threshold description is needed. Initially, critical chloride concentration was considered to be the threshold for the onset of corrosion [12]. Service-life modeling distinguished

between the initiation and the propagation of corrosion process [13]. Studies of steel corrosion in concrete demonstrated the dependence of depassivation on pore solution chemistry and interfacial conditions [14]. Reviews of critical chloride concentration indicate that the threshold is distributed but not deterministic [15]. Comprehensively written corrosion literature also considers the importance of chloride ingress, moisture, oxygen, pore structure, binding and cover depth in concrete corrosion [16]. In such cases, the reduced threshold model is not simply the statement of the perturbation of corrosion by noise but specifies which noises influence corrosion process, how the transport operator filters noise, and at what moment the nonlinear influence leads to the instability of the system.

Fractional diffusion equations are an efficient way to describe non-local or anomalous spreading processes in heterogeneous media. General fractional calculus theory provides the operators for the description of non-local behavior [17]. Fractional differential equation theory extends the scope of these operators to the case of memory and non-classical transport [18]. Theories of anomalous diffusion show how fractional dynamics can describe subdiffusion and long-range transport [19]. Continuous time random walk theory offers another approach to the problem of trapping and fractional evolution [20]. Fractional material response models demonstrate the utility of fractional operators for distributed relaxation and heterogeneous media [21]. Non-classical chloride diffusion in porous media and concrete has motivated the development of fractional and fractal transport models. Initial studies of fractional chloride transport have connected non-Fickian behavior and heterogeneous pore structures [22]. More recent works have related anomalous transport with the tortuosity and binding of pore solution in cement-based materials [23]. Recently developed models also investigated the role of delayed chloride migration in complex concrete microstructure [24]. Fractional and fractal models were also proposed for the representation of scale dependent transport in cracked and porous media [25]. Spectral fractional Laplacian is especially suited for a bounded specimen since the Neumann cosine modes form a natural orthogonal set and each mode is damped by a factor proportional to j^r rather than j^2. This feature is important since when $r < 2$ lower and intermediate spatial modes are not damped in the same way as in the classical diffusion case. Therefore, the modal distribution of environmental fluctuations becomes a part of the corrosion threshold problem.

The second tool needed is the theory of stochastic partial differential equations. Addition of the random forcing on stable modes can change the evolution of a slowly varying mean variable via nonlinear averaging even if the mean mode is not forced directly. Random dynamical systems theory is the general framework for this phenomenon [26]. Slow-fast stochastic analysis explains how rapidly relaxing modes affect the effective drift of slowly varying modes [27]. Stochastic processes theory provides the tools of Ornstein-Uhlenbeck and diffusion theories for this type of reduction [28]. Multiscale theory further formalizes the method of averaging and homogenization for stochastic systems [29]. Infinite dimensional stochastic analysis provides the basis for the analysis of noise driven evolution equations for stochastic PDEs [30]. Modern SPDE theory establishes the necessary existence and regularity framework for SPDEs [31]. Amplitude equation analysis describes how stable modes influence the evolution of slowly varying modes through averaging of moments [32]. Similar is true for the stochastic normal form analysis showing how noise influences slow variables [33]. More recent results generalize this effect to the case of stochastic reaction-diffusion equations [34]. The averaging theory for stochastic evolution equations also provides the rigorous basis for such approximations [35]. This idea is applied to a corrosion activity field in this paper. Central research question is the following: Can fractional diffusion and nonlinear corrosion kinetics turn the additive environmental noise acting on non-mean spatial modes into the explicit thresholds for mean passivation loss or corrosion activity persistence?

The model construction yields a reduced threshold model rather than the electrochemical simulator. The field variable is a normalized activity of corrosion which may represent the intensity of active-state localization, damage activity propensity, pit growth tendency, and coating degradation activity in various applications. This model is scaled to make explicit the coupling between fractional diffusion exponent, diffusion coefficient, modal indices of the force, and the nonlinear kinetics. The derived thresholds are defined by the parameter grid, the modal damping law, and the kinetic closure chosen. This property makes the model useful as a bridge between corrosion mechanisms and practical field measurements of spatial patterns without complete reaction mechanisms.

Another motivation for the use of a reduced activity variable is the difference between mechanistic chemistry of corrosion and field measurements of spatial distributions. Laboratory electrochemical models can describe the electrolyte composition, charge balance, potential gradients and interfacial reactions while inspection data are usually spatial maps with limited chemical resolution. Chloride profiles, half-cell potentials surveys, surface images, acoustic indications, coating holiday maps and tomography derived pore descriptions provide information about the spatial pattern of the process but not the whole reaction mechanisms. Reduced threshold models are useful in this case if they are easily interpretable and assumptions are clear. In this formulation, the reaction law is simplified while the heterogeneity is not treated as an unstructured disturbance but resolved in terms of modal expansion and the effect of each component is filtered by the diffusion operator before entering the mean drift.

For the reinforced concrete, this approach is consistent with the evidence that a single chloride number does not specify the initiation of corrosion [12]. Service-life modeling distinguishes between the initiation and propagation of corrosion and its dependence on transport history and exposure duration [13]. Steel surface conditions and pore solution alkalinity affect the depassivation initiation as well [14]. The review also confirms that moisture, binding and local conditions produce the distributed chloride threshold [15]. For metallic surfaces and coated systems, the localized corrosion depends on the stability of active regions. Pit stability theory describes how local chemistry can prevent repassivation [36]. Pitting corrosion literature highlights the competition between active growth and repassivation [8]. Modern pitting theory also considers the role of geometry and diffusion in this competition [10]. This leads to the model in which the mean mode is not directly forced. If the average environment alone determines the transition then the zero-mean fluctuations will vanish during the spatial averaging. The nontrivial question is if the nonlinear kinetics can retain the influence of these fluctuations after the diffusion filtering. The analysis below answers the affirmative and identifies the retained influence of noise as the variance of modes multiplied by $1/(Dj^r)$.

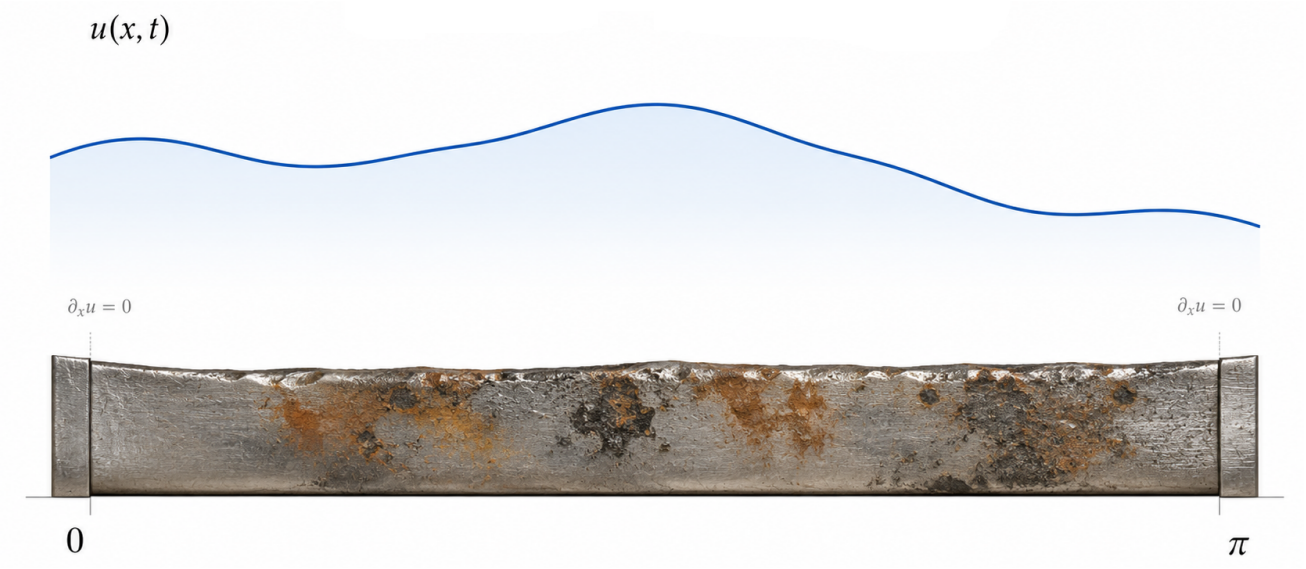

Figure 1: Spectral corrosion interval.

The physical interval associated with the corrosion process is given in Figure 1. A finite trace of the corroded metal or reinforcement surface is identified with $[0, \pi]$, and the no-flux boundary conditions mean that the selected interval is considered as the filtered activity domain. The normalized activity profile plotted above the surface is $u(x, t)$, not the concentration or potential. In this way, the mathematical reduction retains the influence of the environmental variability in the mean activity via the fractional operator and nonlinear reaction terms.

2. Definition of the model and its spectrum

Let $u(x, t)$ be the normalized activity function at the point $x \in [0, \pi]$ at the time $t \geq 0$. The Neumann boundary conditions correspond to the selected material segment without any activity flux from the two endpoints of the selected representative interval. The transport process is assumed to be deterministic, spectral, and fractional. The basis $\{e_0(x) = \pi^{-1/2},\ e_j(x) = \sqrt{2/\pi}\cos(jx),\ j \geq 1\}$ consists of the Neumann eigenfunctions of $-\Delta$, and the fractional operator can be written as

$$(-\Delta)^{r/2} e_0 = 0, \qquad (-\Delta)^{r/2} e_j = j^r e_j, \quad j \geq 1, \tag{1}$$

where $1 < r \leq 2$. If $r = 2$, we have classical diffusion, while lower r makes the gap between low and high modal damping smaller.

From the damping spectrum plotted in Figure 2, one can see the explanation for the fractional correction effect. At $q = 1$ the same exponent leads to the identical value of the modal factor, while the curves become well-separated at $q > 1$. Thus, the role of the fractional order is most pronounced in the case when the corroding heterogeneity possesses the medium and fine scale structures; otherwise, if the process is dominated by the single broad mode, the fractional order plays a negligible role. The stochastic reaction–diffusion equation is given by

$$du = \left[-D(-\Delta)^{r/2} u + f(u)\right] dt + \sum_{j \in \mathcal{J}} \alpha_j e_j(x)\, d\beta_j(t), \tag{2}$$

where $D > 0$ is the diffusion coefficient, f is a reaction law for corrosion-activity, $\mathcal{J}$ is a finite set of forced stable modes, α_j are forcing amplitudes, and $\beta_j(t)$ are independent standard Brownian motions. The forcing has no projection on e_0, so the spatial average is altered only indirectly through nonlinear coupling with stable fluctuations.

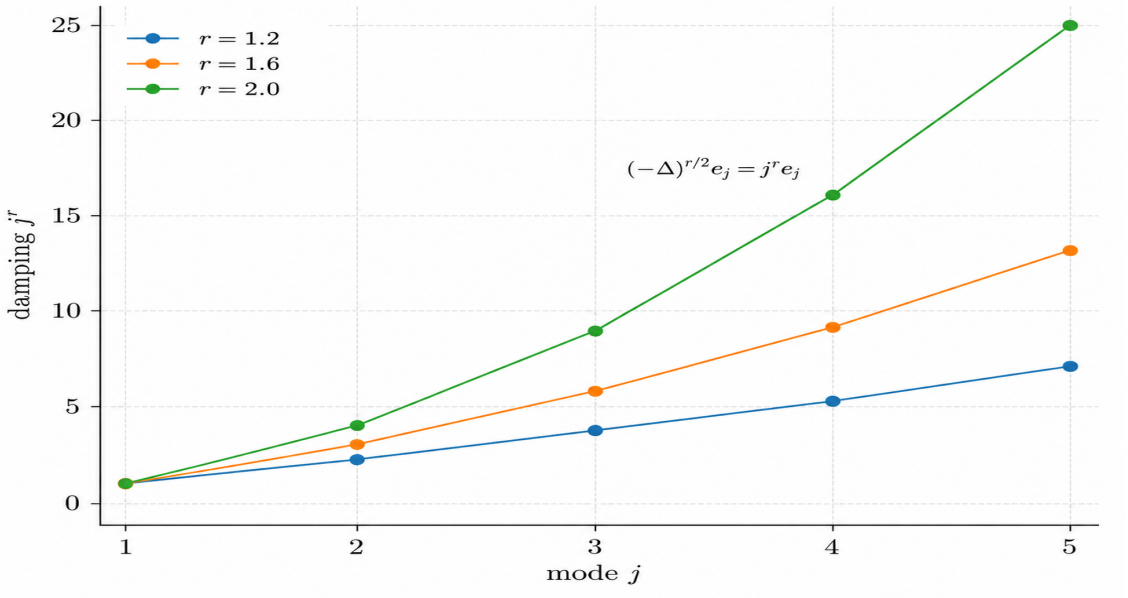

Figure 2: Fractional modal damping.

The finite-dimensional form of the stochastic input is an assumption in the model rather than a convenient mathematical simplification. Real physical corrosion heterogeneity is unlikely to be white in space over the scale of the whole component. It is likely to be structured either by manufacturing artifacts, aggregate distribution, cracks, pores in the coating, wetting paths, inclusions, or exposure gradients. Such structural features have a bounded span of characteristic spatial scales, and a finite set of forced modes provides a straightforward spatial decomposition of measurements or assumptions regarding the heterogeneity. The amplitudes α_j can be interpreted as spectral decomposition coefficients obtained from repeat exposure maps or observed surface structure. The Brownian temporal form models random temporal variations around the prescribed spatial pattern, including humidity fluctuations, splashing, drying out, or renewal of electrolyte.

The choice of the Neumann basis functions also admits an intuitive explanation. The mode e_0 accounts for mean activity, whereas higher-order cosine modes account for increasingly fine deviations from it. In the general multi-dimensional problem the basis will be substituted by the eigenfunctions of the appropriate geometry and boundary conditions, but the mechanism of stability thresholds will stay the same – stable eigenmodes give rise to stationary variance, which enters the mean via the reaction. Thus, the current interval problem is the simplest possible test case to identify the spectral property, which should be preserved in the more complicated geometric setting.

The spectral form is chosen also to avoid any ambiguities related to the meaning of a fractional Laplacian on a bounded domain. There are many nonlocal operators which are sometimes referred to as fractional Laplacians. These operators may have different implications for the behavior of solutions near the boundary. In the current case the fractional Laplacian is constructed as the fractional power of the Neumann Laplacian, so that its eigenmodes and eigenvalues are explicitly known. This allows for reproducible averaging calculation and explicit representation of the damping factor j^r. Extension formulations offer an alternative interpretation of fractional Laplacians in an appropriate setting [37]. Integral and spectral definitions of fractional Laplacians are compared in the broader context of fractional Sobolev spaces [38]. These definitions have their own strengths in various physical contexts; however, their use requires geometry-specific kernels or boundary treatments. The spectral formulation is chosen since the research questions deal with filtering of the spectral modes.

The normalized activity variable is designed to be dimensionless. Zero activity corresponds to a passive or inactive mean state in the reduced description, and positive activity corresponds to increasing corrosion activity or damage tendency. Negative values of the activity variable correspond to the mathematics of the cubic model and do not have a physical meaning of negative corrosion rates. Such choice of coordinates is typical for amplitude equations, where the sign of the reduced coordinate indicates the direction of deviation from a reference state. In a direct implementation of the model in engineering applications, the variable will be mapped onto a nonnegative observable, including active area fraction, normalized corrosion current, pit density index, coating failure index, or depassivation probability. The threshold formulas will be expressed in terms of the calibration of this observable. Rescaling the domain to $[0, \pi]$ is done in order to eliminate unnecessary length constants from the formulas. With the inclusion of the length constant, the denominator in the threshold formula will

include diffusion coefficient, fractional exponent, and the characteristic length of the system. The nondimensionalization isolates the influence of parameters r, D and q on the threshold values. The length constant will appear again when converting the mode index to wavelength in a particular physical application. The mathematical results will remain the same, but the interpretation of a low mode will depend on the geometry. The state is represented as

$$u(x,t) = \xi(t)e_0(x) + \eta(x,t), \qquad \int_0^\pi \eta(x,t)\,dx = 0, \tag{3}$$

where ξ is the mean coordinate responsible for crossing the critical threshold, and η is the stable perturbation. The splitting is not just a convenient mathematical construction. In corrosion terms, ξ characterizes the tendency of the interval to remain passive, become weakly active or sustain some level of damage. The function η describes the spatial deviation from the mean mode and can be interpreted in terms of corrosion hot spots, coating pores, local wetting, microstructural heterogeneities, etc. Since the fractional diffusion operator leaves the mean mode undamped and mode j damped at rate Dj^r, the model has a slow-fast structure, which is needed for spectral averaging.

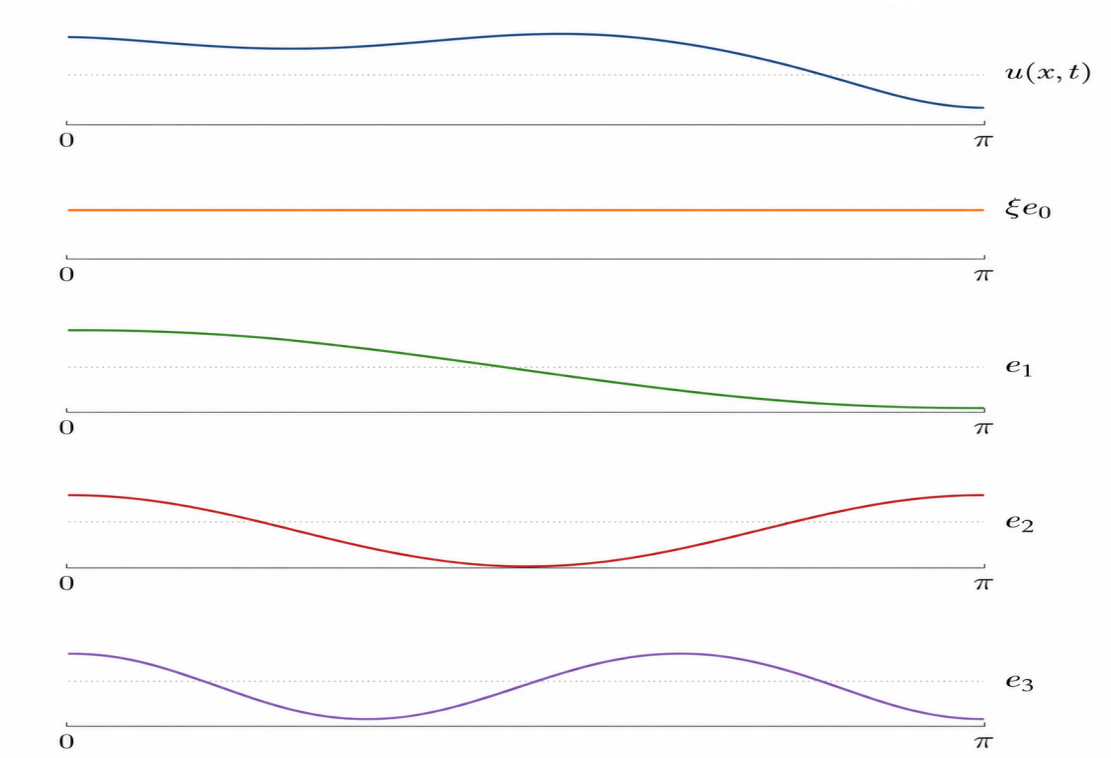

Figure 3: Mean and stable modes.

Modal splitting in Figure 3 shows the difference between the interval-based behavior and spatial deviation from it. The mean mode does not receive direct stochastic forcing; instead, it receives a deterministic correction once the stable modes have been averaged. This implies that for the corrosion problem, any oscillating pattern with zero spatial mean may affect the mean value of activity if the reaction kinetics are nonlinear. The consequence is that statistical inspections of corrosion activity based on either mean chloride concentration or mean coating permeability do not take into account the effect of spatial organization.

Table 1: Parameter grid.

Quantity	Value or role
Domain and boundary condition	$[0,\pi]$ with Neumann boundary condition
Fractional exponent	$r \in \{1.2, 1.6, 2.0\}$
Single forced mode	$q \in \{1,2,3,4,5\}$
Diffusion coefficient	$D \in \{0.5, 1.0, 1.5, 2.0\}$
Cubic stability boundary	$\mathcal{S}_r = 1/3$
Logistic carrying level	$K = 1$ unless otherwise stated
Fast-scale error exponent	$1 - 2m\kappa$ with $m = 3$ and $\kappa = 0.06$

The set of modal and kinetic parameters in Table 1 comprises all of the parameters necessary for calculations. The grid is small on purpose because our intention is not to fit data, but rather to explicitly construct the thresholds. There are three

fractional exponents corresponding to strongly non-classical, intermediate, and classical diffusion. The forced single-mode cases $q = 1$ through $q = 5$ are used to study the effect of spatial scale. The four diffusion coefficients are needed to study the impact of transport filtering on the threshold.

The calculations described in the entries of Table 1 have their own limitations as well. No archives of corrosion exposure are considered, and there are no fitting parameters that are hidden within some opaque calibration procedure. All the listed numbers are calculated based on the modal damping expression, the value of the forcing amplitude, and the selected nonlinearity. The parameters indicate the set of additional measurements required for practical laboratory or field applications – estimations of dominant modes, filtering, and kinetic type are more relevant than one global variance.

3. Averaged mean dynamics

In the regime of fast diffusion, the stable component can be estimated mode-by-mode. For any mode $j \in \mathcal{J}$ forced, the dominant stable variable obeys the Ornstein–Uhlenbeck equation

$$dz_j = -Dj^r z_j \, dt + \alpha_j \, d\beta_j(t). \tag{4}$$

Its stationary mean is zero and its stationary variance is

$$\mathbb{E}z_j^2 = \frac{\alpha_j^2}{2Dj^r}. \tag{5}$$

The modal denominator in Eq. (5) represents the transport filter at the center. It consists of the diffusion constant D that controls the total relaxation rate, and the fractional modal exponent j^r that controls the influence of the spatial frequency on the contribution of the fluctuation to the mean field equation. The total amount of the parameter that enters

$$\mathcal{S}_r = \sum_{j \in \mathcal{J}} \frac{\alpha_j^2}{2Dj^r}. \tag{6}$$

For a single forced mode q, this reduces to $\mathcal{S}_r = \alpha^2/(2Dq^r)$.

The variance channel of Figure 4 defines the probabilistic interpretation of Eq. (5). Stable modes do not grow infinitely due to the action of diffusion, which makes them return to zero. But their stationary amplitude is finite, and its square is exactly the term used in cubic or quadratic averages. Narrowing distribution functions of the higher modes explain why the mean active state coordinate can be influenced by a fluctuating chloride or coating profile with zero mean value, provided that it is multiplied by the fraction of the relaxation rate.

The averaged drift term can be explained by expansion of the reaction law around the mean coordinate and averaging it over the stationary stable field. The odd moments of the stable field vanish within the Gaussian approximation, whereas the second moments remain non-zero. That is why $\mathcal{S}_r$ is the determining quantity within the two closures discussed above. Higher order closures would result in introduction of the fourth and higher moments, but the second moment term would still be the first correction to the mean equation due to zero-mean additive fluctuations. The reduction procedure is thus not an artificial addition of the noise penalty term.

The sign of the correction depends on the curvature and higher-order derivatives of the reaction law. From the point of view of corrosion processes, this implies that the spatial heterogeneity, by itself, is neither good nor bad – its averaged impact is defined through the dynamics of the local kinetics in response to deviation from the average value. Convex, saturating and bistable reaction law can generate different scalars depending on the chosen $\mathcal{S}_r$. The purpose of considering two different closures is to illustrate this dependency.

The fast-diffusion assumption should be understood as the scale separation between spatial relaxation and mean evolution. It does not postulate infinite diffusion, nor does it disregard the significance of local gradients. It states that the forced stable coordinates acquire their stationary distribution at such times that the mean coordinate experiences their averaged variance. The scale separation of slow-fast stochastic systems offers the basic justification for this assumption [27]. Multiscale averaging formalises the procedure of averaging of rapidly relaxing coordinates [29]. The techniques of stochastic normal forms demonstrate how small-scale variables can affect the drift of a slow variable although they have no mean value [33]. With respect to corrosion applications, the hypothesis is more reasonable when the spatial heterogeneity is perturbed around a slowly varying damage state than when the damage development is governed by abrupt cracking, delamination or pit coalescence. The projection of Eq. (2) onto the mean mode results in the deterministic drift that can be represented as an averaged value of the reaction law $f(\xi e_0 + \eta)$. Neglecting the odd-moments contribution and keeping only up to the first even moment, one can write the equation for the mean coordinate in the form

$$\dot{\xi} = \bar{f}(\xi; \mathcal{S}_r). \tag{7}$$

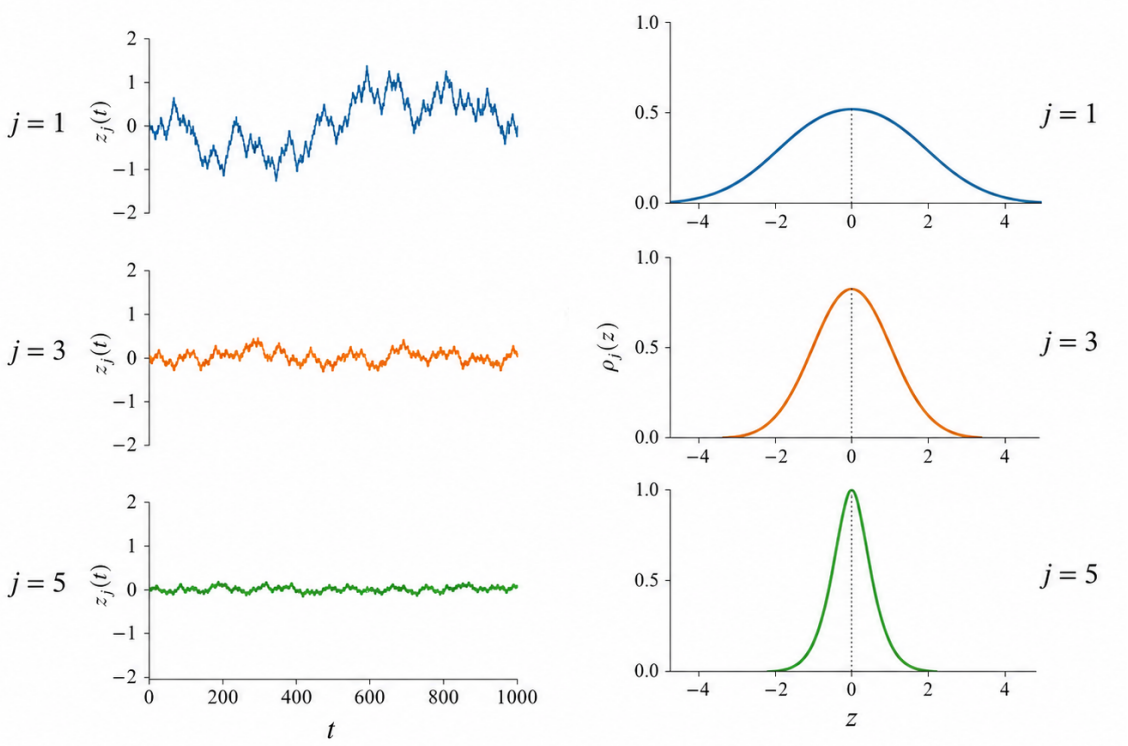

Figure 4: Stable-mode variance.

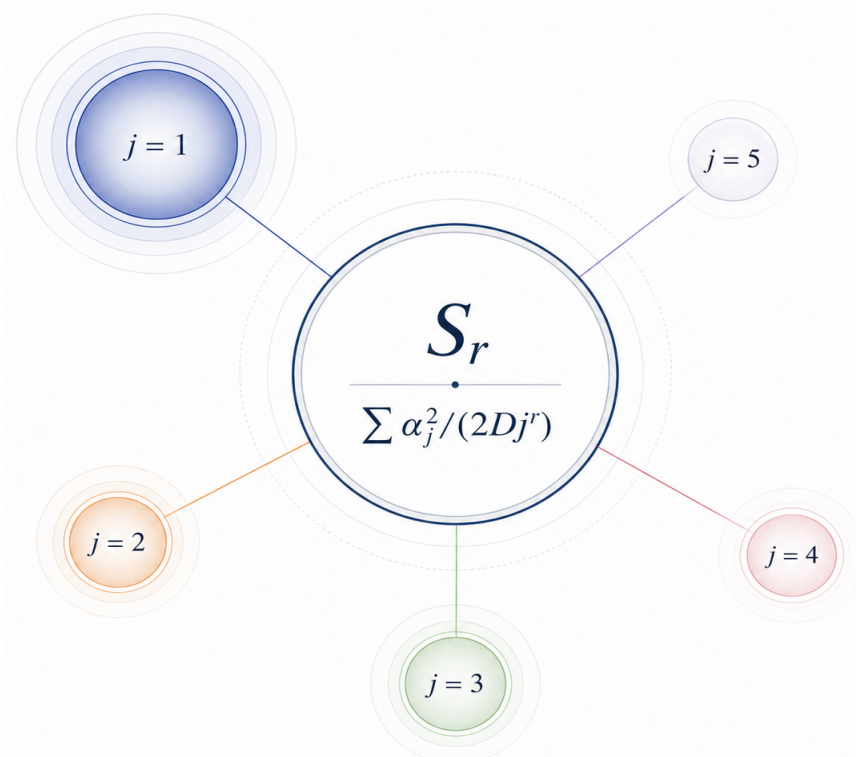

Figure 5: Filtered spectral strength.

Two different closures are considered due to their answering different corrosion problems. The cubic passivation–activation kinetics help to understand whether the passive state inhibits small activity. The logistic damage-growth kinetics enable us to check whether there exists a steady-state activity level beyond spatial heterogeneity averaging. Analytical background of the reduced parabolic PDEs can be found in semigroup theory [39]. The study of the behaviour of infinite-dimensional dynamical systems gives another background for modal reductions [40]. Reaction–diffusion modelling explains the connection of cubic reaction law with bistability and amplitude saturation [41]. The nonlinear parabolic equations theory confirms the possibility of using reduced polynomial kinetics [42]. Logistic law will be considered as the simplest example of self-limiting growth.

Figure 5 shows the spectral strength visual which filters out the scalar variable that gets carried forward in the threshold

computations. The first mode will have the maximum radius since it is less damped compared to other modes. Modes above it add lesser amounts for the same magnitude of force since their damping effect becomes increasingly significant. What we need to know is that $\mathcal{S}_r$ is not the unweighted variance of the forcing but the variance after diffusion.

4. Passivation and persistence thresholds

The cubic passivation–activation closure is

$$f(u) = u - u^3. \tag{8}$$

Averaging over the stable field and retaining the leading variance correction gives

$$\dot{\xi} = (1 - 3\mathcal{S}_r)\xi - \xi^3. \tag{9}$$

The passive state $\xi = 0$ is linearly stable if $1 - 3\mathcal{S}_r < 0$, which gives

$$\mathcal{S}_r > \frac{1}{3}. \tag{10}$$

It possesses a simple corrosion-based interpretation. The linear growth rate of the average activity is reduced when averaged within the cubic closure due to fluctuations. For sufficiently intense fluctuations, the passive state is stabilized. One should not view this result as implying that environmental noise is always beneficial. It is a characteristic feature of the cubic closure in which the nonlinear part of the equation penalizes deviations via the third-order term.

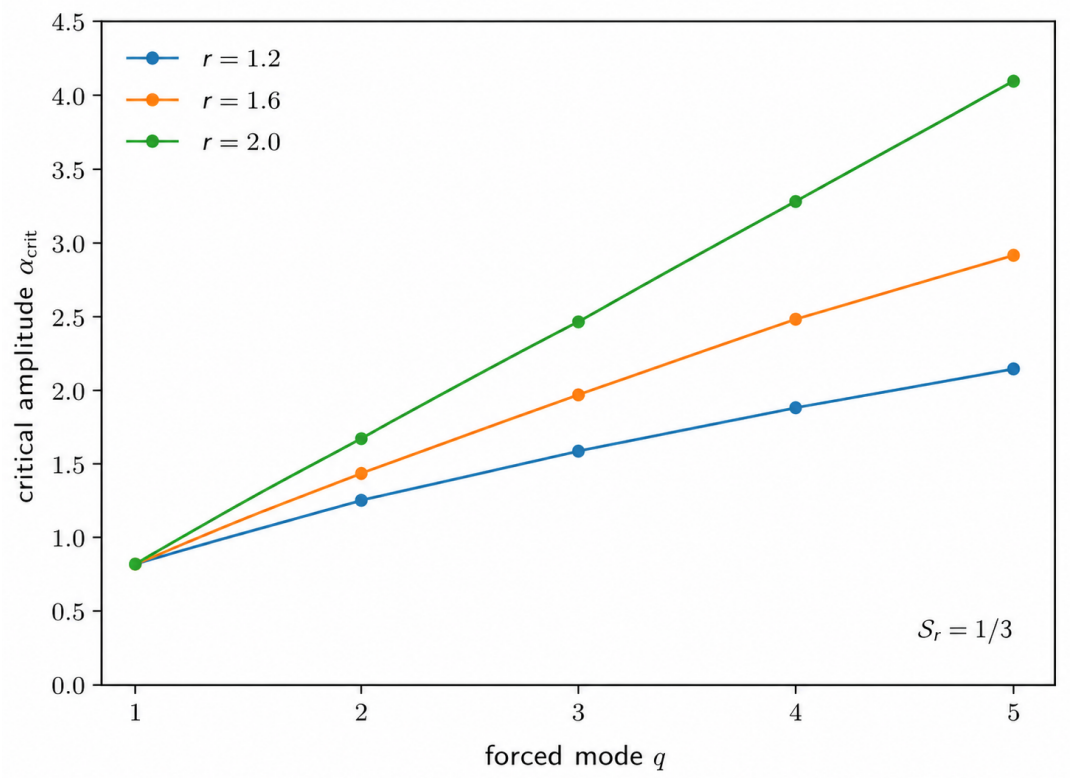

Figure 6: Cubic passivation threshold.

The curve shown in Fig. 6 demarcates the range of amplitudes whose forcing leaves small activity unstable and the region whose amplitudes fulfill the cubic passivation condition. For one mode of forcing, the critical level is given by Eq. (10) to be

$$\alpha_{\text{crit}} = \sqrt{\frac{2Dq^r}{3}}, \tag{11}$$

so that larger D, larger q, and larger r all demand stronger forcing in order to obtain an equivalent average effect on stability. The most significant case is thus not the most noisy, but the case that puts variance into slowly damped modes.

The drift functions in Fig. 7 make the meaning of the algebraic threshold dynamical. For $\alpha < \alpha_{\text{crit}}$, the origin is unstable and there may be nonzero steady-state solutions that attract trajectories near to zero; for $\alpha > \alpha_{\text{crit}}$, trajectories near the origin are driven towards passivity. In physical terms, the cubic theory thus predicts a regime where variance in spatial averages makes the average passive state more stable, but only when the variance crosses a certain spectral threshold.

The logistic closure for damage growth is

$$f(u) = u(K - u), \qquad K > 0. \tag{12}$$

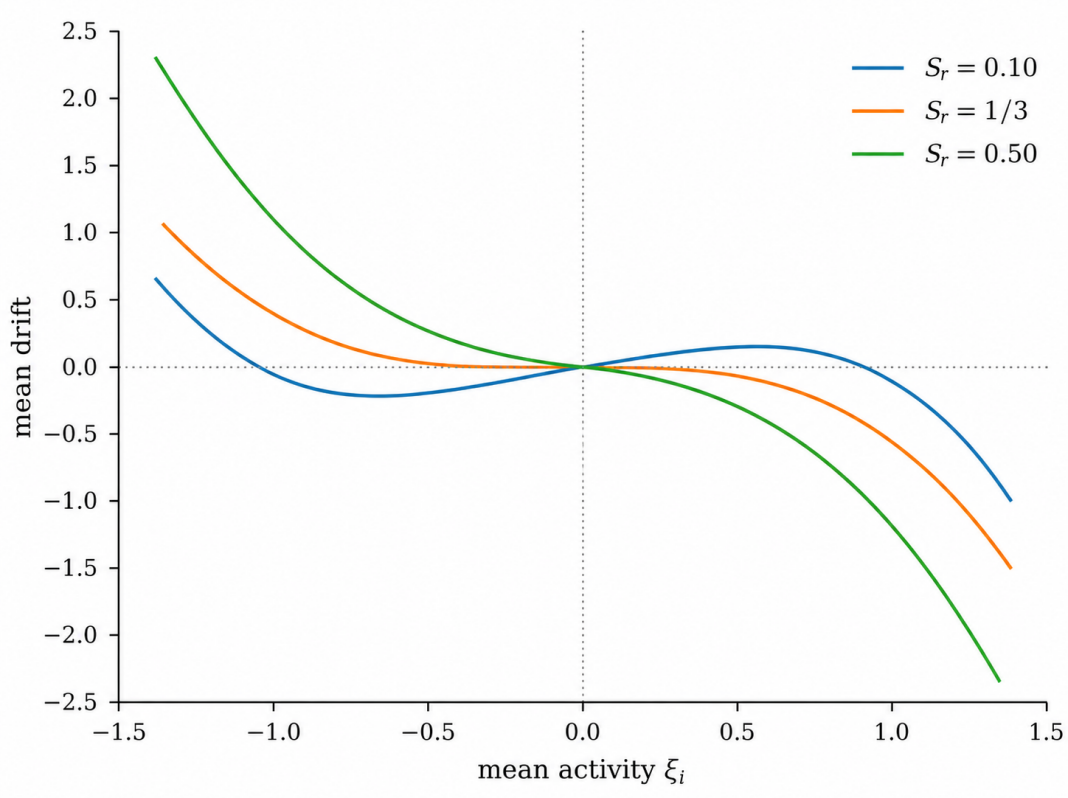

Figure 7: Cubic mean drift.

The averaged mean equation becomes

$$\dot{\xi} = \xi(K - \xi) - \mathcal{S}_r. \tag{13}$$

The equilibria satisfy

$$\xi_{\pm} = \frac{K \pm \sqrt{K^2 - 4\mathcal{S}_r}}{2}, \tag{14}$$

so positive real equilibria exist only when

$$\mathcal{S}_r \leq \frac{K^2}{4}. \tag{15}$$

This is not the same result as the cubic one. The effect of stochastic correction causes the logistic curve to be shifted down, thus eliminating the positive stationary state. Two stationary states are observed when $\mathcal{S}_r$ is small; their merger is observed at $K^2/4$; above this level, no positive stationary state is found for the modified logistic balance. If the parameter ξ is understood as the property of permanent damage, then the threshold corresponds to losing such a stationary state.

Table 2: Kinetic thresholds.

Closure	Averaged mean equation	Threshold	Interpretation
Cubic passivation–activation	$\dot{\xi} = (1 - 3\mathcal{S}_r)\xi - \xi^3$	Passive mean is stable when $\mathcal{S}_r > 1/3$	Small activity decays
Logistic damage growth	$\dot{\xi} = \xi(K - \xi) - \mathcal{S}_r$	Positive equilibria require $\mathcal{S}_r \leq K^2/4$	Sustained activity persists only below boundary

As seen from the equilibrium branches in Figure 8, filtered variance tends to reduce the positive activity domain. It should be noted that it is not implied by this approach that there would be no more corrosion when there is any random exposure. According to the logistic closure, the equation for the mean loses its positive deterministic balance due to the fact that heterogeneity provides an averaging negative offset large enough.

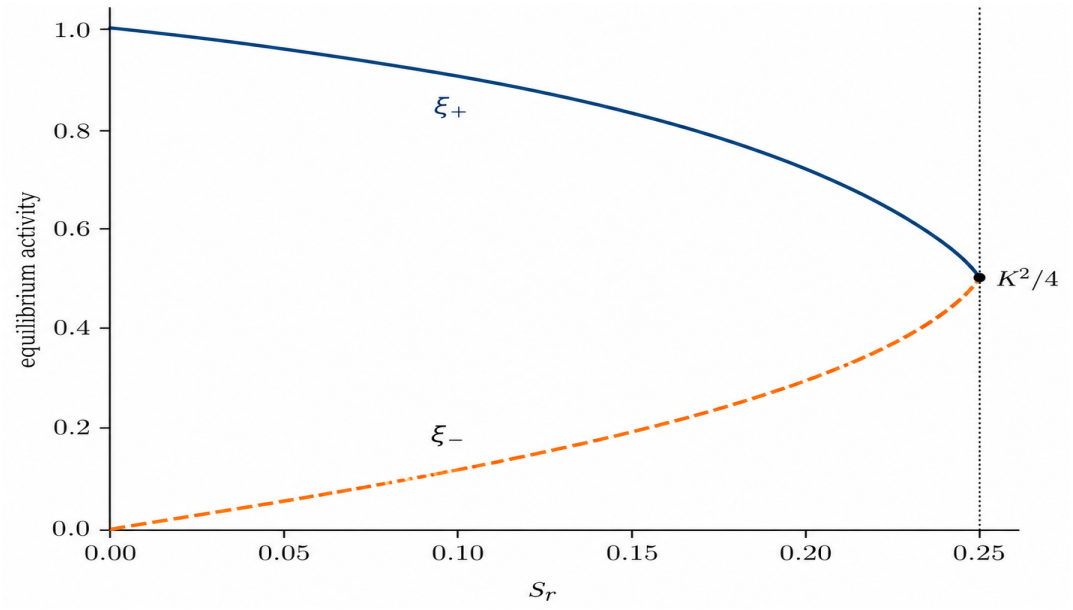

Figure 8: Logistic persistence boundary.

The comparison presented in Table 2 helps to avoid an easy misunderstanding related to the model. The random term does not have any universal sign other than the kinetic closure defining it. What does not change when passing from one closure to the other is the spectral intensity $\mathcal{S}_r$. The scalar being evaluated from the modal information, it will be possible to explore different hypotheses about the corrosion by using different reaction functions. This separation is valuable because coating degradation, pitting stability, and reinforced-concrete corrosion may not share the same reduced kinetics.

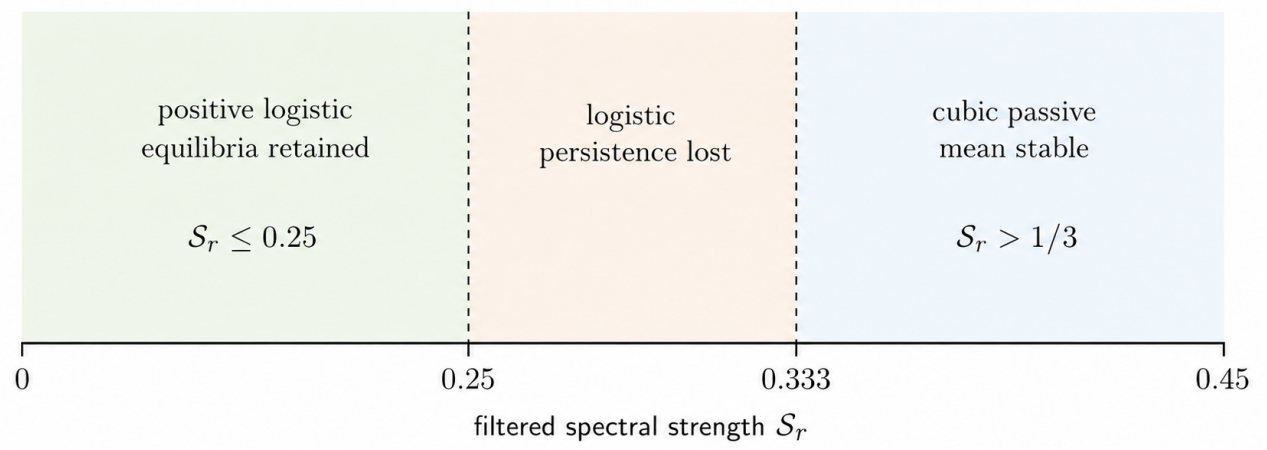

Figure 9: Kinetic threshold comparison.

As shown by the scalar comparison in Figure 9, the two closures intersect the spectral-strength axis at distinct locations. In the case of $K = 1$, logistic persistence fails at the value 0.25, while cubic passivation of the mean occurs only at 1/3. The region between these two values thus is not ambiguous: it represents the area of kinetic dynamics in which the logistic persistence condition is no longer satisfied, while the cubic passivation of the mean still has not occurred.

5. Results and discussion

The numeric results can be interpreted as sensitivities associated with the threshold equations. For the cubic closure and a single forced mode with $D = 1$, the critical amplitudes resulting from Eq. (11) are shown in Table 3. It can be seen that, in each case, the amplitudes increase with increasing q due to the increased dissipation rate of higher modes. This growth is relatively small at $r = 1.2$ and quite large at $r = 2.0$. For instance, at $q = 5$, the critical amplitudes are equal to 2.148 at $r = 1.2$ and 4.082 at $r = 2.0$. Thus, classical diffusion makes fine-scale fluctuations much less able to influence the mean than fractional diffusion does.

Table 3: Amplitude thresholds.

Forced mode q	$r = 1.2$	$r = 1.6$	$r = 2.0$
1	0.816	0.816	0.816
2	1.238	1.422	1.633
3	1.579	1.968	2.449
4	1.877	2.475	3.266
5	2.148	2.935	4.082

The values listed in Table 3 address a practical design issue. If a corrosion protection system is characterized by widespread areas of spatially variable environments, then a small amplitude is enough to cause mean-field dynamics. When the same variance is divided into smaller spatial fluctuations, then the critical amplitude increases. It is important to keep this aspect in mind when working with the inspection maps. A surface that contains some widely spread regions of chloride concentration will produce a greater impact on mean activity than a surface with many small isolated fluctuations.

The weights of the modes in Table 4 provide a direct explanation of the aforementioned feature. The first mode is always characterized by the unity relative weight, whereas the fifth mode has only 0.145 times that value at $r = 1.2$, and only 0.040 at $r = 2.0$. Therefore, the exponent r can be viewed as a selectivity parameter.

Table 4: Modal weights.

Mode j	$j^{-1.2}$	$j^{-1.6}$	$j^{-2.0}$
1	1.000	1.000	1.000
2	0.435	0.330	0.250
3	0.268	0.172	0.111
4	0.189	0.109	0.063
5	0.145	0.076	0.040

From Table 4, it is clear how the model can be applied for imaging or monitoring applications. A map of the chlorides, impedance, or damage can be expanded in terms of spatial modes and the weights on each of the modes can be the respective fractional damping value. The weighted variance provides more information about the reduced mean dynamics than the unweighted variance. This is because the low spatial frequencies may contain important information and smoothing may eliminate them.

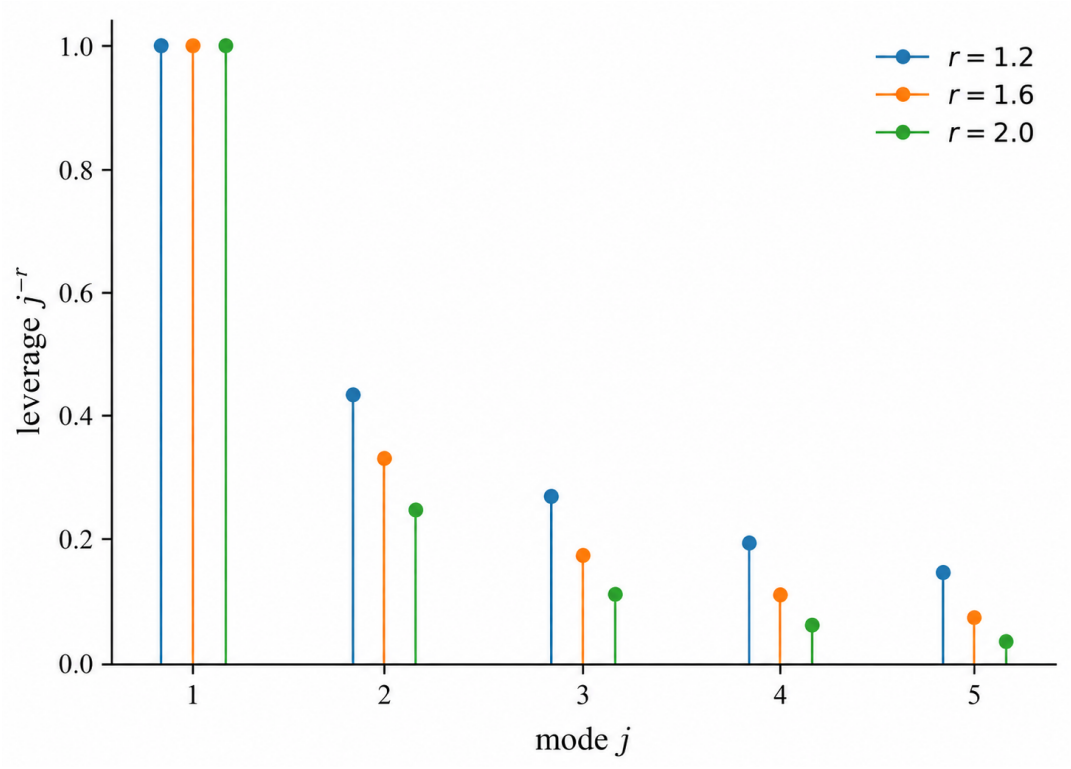

Figure 10: Modal leverage.

Indeed, the same statement can be visually illustrated using the lollipop plot of Figure 10, where we can see that the leverage of the first mode remains constant at one, while the leverage of the fifth mode goes down to 0.145, 0.076, and 0.040,

when r rises from 1.2 to 2.0. The successive collapse of the high mode leverage explains numerically why wide patches of chloride or defect bands can control the mean response, even though the small-scale textures look very irregular.

The impact of diffusion on the threshold is determined by the presence of D^{-1} in $\mathcal{S}_r$ and $\sqrt{D}$ in the critical amplitude. In the particular case of $q = 2$, $r = 1.6$, and cubic critical amplitudes are listed in Table 5. Increasing D from 0.5 to 2.0 leads to the increase of α_{crit} from 1.006 to 2.011. Thus, higher transport filtering increases the resistance of a material to the influence of spatial fluctuations on the mean activity.

Table 5: Diffusion shift.

Diffusion coefficient D	α_{crit} for $q = 2$, $r = 1.6$
0.5	1.006
1.0	1.422
1.5	1.741
2.0	2.011

The behavior exhibited in Table 5 allows for a concise interpretation in terms of materials design. Coatings, microstructures, or concrete coverings that reduce long-distance-connected transport will reduce the diffusion of activity and thus will result in heterogeneity becoming more important. On the other hand, systems that reduce spatial gradients will be less sensitive to periodic perturbations of the same magnitude. The model is not making an argument that larger diffusion will always lead to increased durability, since it can diffuse aggressive species as well.

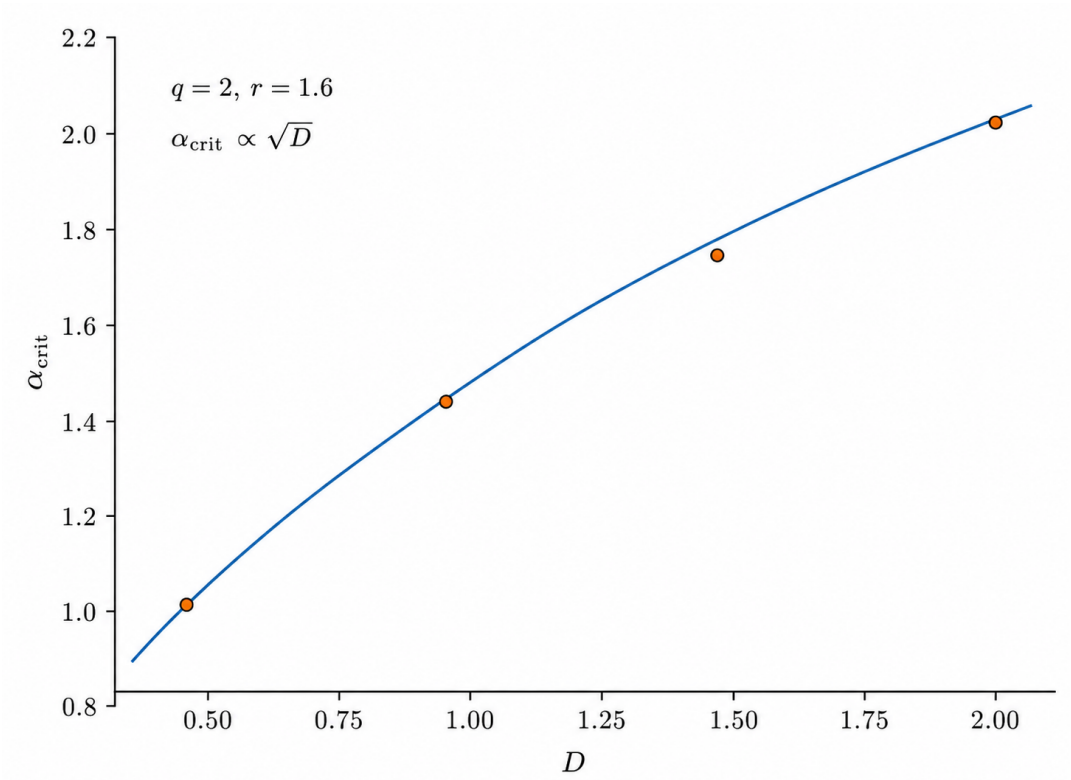

Figure 11: Diffusion scaling.

The scaling demonstrated in Figure 11 illustrates in addition to the numerical values that the critical amplitude scales as a square root of D. Such dependence is convenient for calibration purposes as it does not require any artificial fit to be performed. When the dominant mode and the fractional exponent are determined, the diffusion dependence of the critical amplitude can be calculated using the Eq. (11). Therefore, the model provides a small parameter analysis: the uncertainty in D leads to predictable uncertainty in the amplitude necessary to change the passive state stability.

The applicability of the fast-scale approximation is guaranteed when the relaxation rate of stable modes is substantially higher than the average value. For $m = 3$ and $\kappa = 0.06$ the remainder exponent $1 - 2m\kappa$ is equal to 0.64. The positive remainder exponent means that the remainder of the expansion decreases with decreasing the scale parameter. The key point here is not in the exactness of the averaged equation, but in its asymptotic properties, which become better in case of increasing time-scale separation and small amplitudes of the stable modes.

The behavior of the remainder term demonstrated in Figure 12 is essential to apply the obtained formulas for the calculation of the threshold values properly. In case of insufficiently fast damped modes, sufficiently high amplitudes (such

that the higher-order moments start to dominate), or different kinetic processes (which deviate substantially from the adopted cubic and logistic forms of the nonlinearity), the threshold values have to be considered as qualitative estimates only.

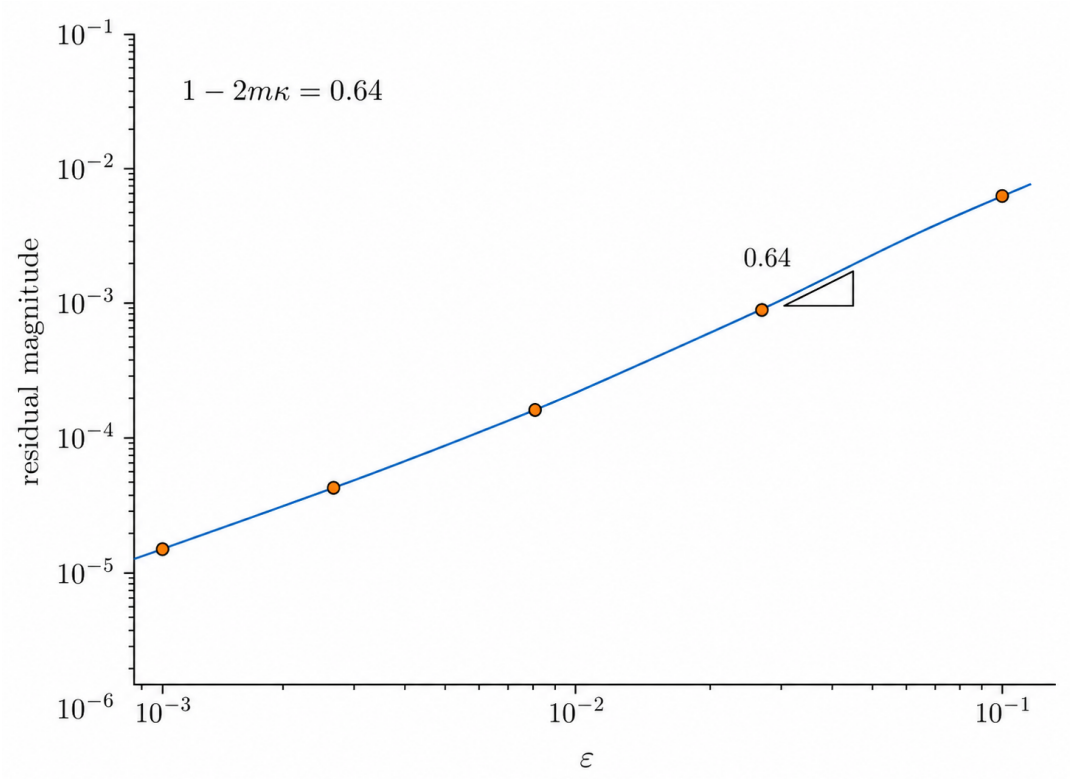

Figure 12: Remainder decay.

The two kinetic closures yield distinct types of interpretation for the engineering applications. In the cubic closure, the average variance can stabilize the passive mean state. This can be interpreted as a passivating feedback where deviations from the mean state are penalized more strongly than they are amplified. In the logistic closure, the same spectral strength opposes the growth balance and eliminates the possibility of positive equilibria. In both of the cases, the environmental fluctuation influences the dynamics through nonlinear averaging and not the mean forcing. According to pit-stability theory, the sustained local transport and chemistry control the activity [36]. In pitting corrosion, the relevant nucleation, metastability and stable growth stages are distinguished [8]. Chloride threshold analysis in concrete indicates that the depassivation depends on the definition of the chloride content [43]. Other studies confirm that threshold conditions depend on the concrete-steel state and exposure variables [44]. In the critical review, it is stated that the concrete-steel depassivation cannot be described by a universal reaction law [15]. Therefore, the distinction between the two closures is important for studying the pit nucleation, pit stability, underfilm spreading and depassivation of concrete-steel.

One more conclusion is that data reduction should be spectral rather than statistical. Variance, standard deviation and coefficient of variation are not sufficient when the transport is fractional since the same statistical variance can be allocated differently. The threshold variable $\mathcal{S}_r$ combines the amplitude, spatial scale, damping factor and diffusion coefficient into one value. That is why the parameters grid focuses on q, r and D rather than just on the noise intensity. For the image-based corrosion assessment, the technique implies projection of the measured heterogeneity on a physical basis and weighting of the coefficients before calculating the mean activity.

The threshold tables demonstrate that the fractional order cannot be considered as a minor technical modification of the classical diffusion equation. At $q = 1$, all three exponents give the same critical amplitude since $1^r = 1$. The differences start to appear when the forcing has spatial structure at higher modes than one. This means that estimation of r from spatial data is most helpful when the corrosion map has several scales of active patterns. When a specimen is dominated by the one broad exposure gradient, the fractional exponent will be hard to estimate from the threshold properties. In case it is dominated by multiple medium scales, the exponent significantly influences their relative weight.

A good way to interpret the results is to compare two surfaces with equal total forcing amplitude. On the first surface, most of the variability is located at $q = 1$ or $q = 2$, which corresponds to the broad wetting and chloride patches. On the second surface, the variability is split between $q = 4$ or $q = 5$, corresponding to the speckled irregularity. The reduced model predicts that the first surface has a stronger impact on the mean activity, since its variance is less strongly damped. This conclusion is not available using the ordinary variance computation. It can be obtained only after the spatial spectrum

has been weighted using the fractional transport operator.

The logistic threshold brings additional information about the problem. At $K = 1$, the persistence boundary is $\mathcal{S}_r = 0.25$, which is lower than the cubic stability boundary $\mathcal{S}_r = 1/3$. Thus, in terms of the nondimensional normalization used here, the logistic positive-equilibrium condition fails before the cubic passive-state boundary is exceeded. This discrepancy does not contradict anything. It is related to the fact that the two closures consider different questions. The cubic calculation checks if the activity close to zero is stable. The logistic calculation checks if the positive equilibrium is available. These two experiments correspond to the two different endpoints in material study: repassivation of the low-level activity or maintenance of the sustained damage rate.

Since the thresholds are explicit, they can be used in sensitivity analysis. Suppose the dominant mode is known, but D and r are unknown. Then the formula for α_{crit} reveals how the uncertainties propagate: errors in D are entered in a square root, and errors in r enter the q^r logarithmically. It means that uncertainty in the exponent has negligible effect at $q = 1$ but significant at higher modes. In practice, the scale of the dominant exposure pattern has to be estimated before the threshold can be calculated with confidence. The model also provides a conservative way to compare the classical and fractional transport. At $r = 2$, the high-order modes are fast-decaying, and the broad features dominate the mean correction. At $r = 1.2$, the mode attenuation is slower, and the intermediate modes have a stronger influence. Anomalous diffusion theory explains how the heterogeneous media can sustain the nonclassical transport effects [19]. The fractional diffusion models describe the probabilistic and analytical approach to the nonlocal connectivity [45]. The fractional Sobolev theory reveals the operator structures responsible for the slower modal attenuation [38]. For the chloride-bearing porous media, the inference is that the correct exponent identification can be as important as the diffusion coefficient.

The threshold values show how the multi-mode forcing will act. Although the tables are presented for single-mode thresholds, Eq. (6) is additive in the forced set $\mathcal{J}$. Thus, several subcritical modes can interact to exceed a threshold even if none of the individual modes is large enough. This is important for the actual corrosion maps, since the exposure heterogeneity is rarely represented by a single wavelength. The broad wetting mode, the coating defect mode and the pore connectivity mode can each have modest variances. Their sum may still bring the mean dynamics over the cubic or logistic boundary. On the other hand, many high-order modes can make insignificant contribution if their sum is small.

The additivity of $\mathcal{S}_r$ provides a useful ranking algorithm. Each measured or simulated modal coefficient can be transformed to the contribution $\alpha_j^2/(2Dj^r)$, and the highest contributions can be kept for interpretation. In this way, the detailed spatial field is not overfitted, but the features relevant to the reduced mean dynamics are preserved. Also, this provides a sensible way to compare mitigation strategies. Repair that decreases the amplitude of the first two modes will have much larger effect on the threshold state than removal of the fine-scale roughness but leaving the broad chloride heterogeneity unchanged.

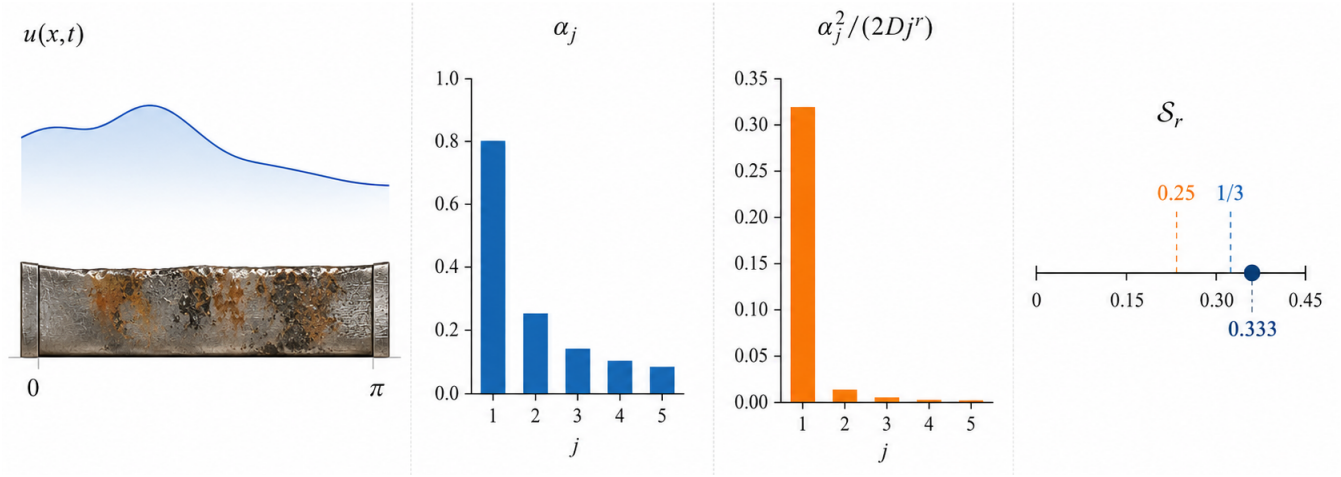

Figure 13: Spectral threshold reading.

Figure 13 presents the synthesis of the visual corrosion field and the numeric threshold calculation. Namely, the spatial activity profile is presented via its modal amplitudes, amplitudes are transformed into filtered modal contributions, and the sum is placed on the $\mathcal{S}_r$ axis. As one can see, this last observation clarifies the reasoning behind the fact that the threshold decision is made based on information beyond the mere image.

The result itself is best understood as a transparent reduction rather than a universal law of corrosion. Namely, the model provides a mathematically exact path from the spatial variability to the mean activity, but the kinetic closure is based on certain physical assumptions. The cubic law is correct in case of the presence of the nonlinear restoring effect due to passivation or saturation; the logistic law is correct in case of the growth of activity at small values of intensity

and limitation at large values of intensity. The experimental use of the model therefore needs to start with establishing which endpoint is modeled. Having chosen the endpoint, the same spectral calculation can be done to determine whether the measured heterogeneity is dynamically important. The model suggests the direct way for validation. Namely, one can measure a sequence of spatial exposure maps, transform each of them into the modal coefficients either using the cosine basis or the eigenbasis of a particular geometry, estimate α_j^2 based on the temporal variance of each coefficient, and calculate $\mathcal{S}_r$ for a certain set of D and r. Then one can compare the predicted threshold state with the measured transition indicators such as pit stability, fraction of active area, local corrosion current stability, or depassivation events. Such a validation will not require matching all the details of the reduced model to the data; instead, it will confirm the narrow claim of the present study: the spectral variance weighted by the transport effects gives better prediction of the mean activity transitions than the plain variance or the mean exposure.

The second application of the model is the numerical experiment design. Namely, the full corrosion simulations can be costly when resolving chemistry, transport, and morphology. The reduced thresholds will allow to identify the spatial forcing cases that need to be simulated in high fidelity. The cases close to the boundaries $\mathcal{S}_r = 1/3$ and $\mathcal{S}_r = K^2/4$ are much more informative than the cases far away from any boundary because they show how sensitive is the threshold to the kinetic details. In that sense, the model works as a screening theory. Namely, it narrows the parameter space prior to using a detailed simulator or performing an experiment to investigate the electrochemical mechanisms. The limitations of the model are equally clear. The interval geometry is one-dimensional, the noise is additive and finite-dimensional, the boundary condition is Neumann, and the kinetics are reduced scalar closures. The model is not resolving electric potential, chemical speciation, pit solution chemistry, rust layer evolution, crack opening, or mechanical stress. Therefore, it needs to be considered as a threshold theory for the patterned activity and not as the general-purpose corrosion simulator. In that sense, the value of the model is maximized when the scientific question is the following: is the spatially filtered heterogeneity able to change the mean activity, and the available data supports the modal or spectral representations of the variability better than the full multiphysics parameterization.

6. Conclusion

The question asked was the following: can spatially structured fluctuations, acting on stable non-mean modes, change the mean corrosion activity of a fractional reaction–diffusion system via nonlinear averaging? The answer is yes, provided that the filtered spectral strength is large enough compared to the kinetic threshold. Namely, the decisive scalar is

$$\mathcal{S}_r = \sum_{j \in \mathcal{J}} \frac{\alpha_j^2}{2Dj^r}.$$

The latter quantity is not the unweighted noise variance. Instead, it is the transport-weighted variance, and it shows why the low spatial modes can dominate the mean response.

For the cubic passivation-activation kinetics, the passive mean state becomes linearly stable if $\mathcal{S}_r > 1/3$. For the logistic damage-growth kinetics, the positive persistent equilibrium exists if and only if $\mathcal{S}_r \leq K^2/4$. As one can see from the numerical threshold table, the amplitude necessary to reach the cubic boundary grows with the mode number, diffusion coefficient, and the fractional exponent. For instance, at $D = 1$, the critical amplitude for $q = 5$ increases from 2.148 at $r = 1.2$ to 4.082 at $r = 2.0$, while the first mode threshold is equal to 0.816 for all exponents. At $q = 2$ and $r = 1.6$, increasing the diffusion coefficient from 0.5 to 2.0 leads to the increase in the critical amplitude from 1.006 to 2.011. These examples illustrate the effect of the mode placement and the transport filtering in the determination of the dynamic importance of the environmental heterogeneity.

Based on the fact that the derivation is done in modal variables, the result is portable to different spatial measurements. Whether the heterogeneity is obtained from laboratory imaging, service inspection, or deterministic numerical forcing fields, the following sequence takes place: identify the dominant spatial modes, weigh them using the fractional damping law, and compare the resulting $\mathcal{S}_r$ to the kinetic boundary corresponding to the corrosion endpoint. The modal representation of the result allows transforming the spatial variability into the threshold variable with physical meaning.

References

[1] Fontana, M. G. (1985). Corrosion engineering.
[2] Jones, D. A. (1996). Principles and prevention of corrosion. (No Title).
[3] Silman, H. (1972). Corrosion and Corrosion Control: An introduction to corrosion science and engineering.
[4] Marcus, P., & Oudar, J. (Eds.). (2002). Corrosion mechanisms in theory and practice (pp. 243-286). New York: Marcel Dekker.
[5] Bard, A. J., & Faulkner, L. R. (2001). Electrochemical methods: fundamentals and applications, John Wiley & Sons. Inc., New York, 60-62.
[6] Newman, J., & Thomas-Alyea, K. E. (2004). Electrochemical Systems, Wiley.
[7] Landolt, D. (2007). Corrosion and surface chemistry of metals. EPFL press.

[8] Frankel, G. S. (1998). Pitting corrosion of metals: a review of the critical factors. Journal of the Electrochemical society, 145(6), 2186-2198.
[9] Frankel, G. S., & Sridhar, N. (2008). Understanding localized corrosion. Materials today, 11(10), 38-44.
[10] Newman, R. (2010). Pitting corrosion of metals. The Electrochemical Society Interface, 19(1), 33-38.
[11] Li, T., Wu, J., & Frankel, G. S. (2021). Localized corrosion: Passive film breakdown vs. Pit growth stability, Part VI: Pit dissolution kinetics of different alloys and a model for pitting and repassivation potentials. Corrosion Science, 182, 109277.
[12] Hausmann, D. A. (1967). Steel corrosion in concrete–How does it occur?. Materials protection.
[13] Tuutti, K. (1982). Corrosion of steel in concrete.
[14] Page, C. L., & Treadaway, K. W. J. (1982). Aspects of the electrochemistry of steel in concrete. Nature, 297(5862), 109-115.
[15] Angst, U., Elsener, B., Larsen, C. K., & Vennesland, Ø. (2009). Critical chloride content in reinforced concrete—A review. Cement and concrete research, 39(12), 1122-1138.
[16] Bertolini, L., Elsener, B., Pedeferri, P., Redaelli, E., & Polder, R. B. (2013). Corrosion of steel in concrete: prevention, diagnosis, repair. John Wiley & Sons.
[17] Kilbas, A. A., Marichev, O. I., & Samko, S. G. (1993). Fractional integrals and derivatives (theory and applications).
[18] Podlubny, I. (1998). Fractional differential equations: an introduction to fractional derivatives, fractional differential equations, to methods of their solution and some of their applications (Vol. 198). elsevier.
[19] Metzler, R., & Klafter, J. (2000). The random walk's guide to anomalous diffusion: a fractional dynamics approach. Physics reports, 339(1), 1-77.
[20] Barkai, E., Metzler, R., & Klafter, J. (2000). From continuous time random walks to the fractional Fokker-Planck equation. Physical review E, 61(1), 132.
[21] Mainardi, F. (2010). Fractional calculus and waves in linear viscoelasticity, Imperial College Press, London.
[22] Chen, W., Sun, H., Zhang, X., & Korošak, D. (2010). Anomalous diffusion modeling by fractal and fractional derivatives. Computers & Mathematics with Applications, 59(5), 1754-1758.
[23] Wei, S., Chen, W., & Zhang, J. (2017). Time-fractional derivative model for chloride ions sub-diffusion in reinforced concrete. European Journal of Environmental and Civil Engineering, 21(3), 319-331.
[24] Chen, R., Wei, X., Liu, F., & Anh, V. V. (2020). Multi-term time fractional diffusion equations and novel parameter estimation techniques for chloride ions sub-diffusion in reinforced concrete. Philosophical Transactions of the Royal Society A: Mathematical, Physical and Engineering Sciences, 378(2172).
[25] Feng, C., Si, X., Li, B., Cao, L., & Zhu, J. (2021). An inverse problem to simulate the transport of chloride in concrete by time–space fractional diffusion model. Inverse Problems in Science and Engineering, 29(12), 2429-2445.
[26] Arnold, L. (2006). Random dynamical systems. In Dynamical Systems: Lectures Given at the 2nd Session of the Centro Internazionale Matematico Estivo (CIME) held in Montecatini Terme, Italy, June 13–22, 1994 (pp. 1-43). Berlin, Heidelberg: Springer Berlin Heidelberg.
[27] Berglund, N., & Gentz, B. (2006). Noise-induced phenomena in slow-fast dynamical systems: a sample-paths approach. London: Springer London.
[28] Gardiner, C. W. (2009). "Stochastic methods: A handbook for the natural and social sciences". Springer Berlin.
[29] Pavliotis, G., & Stuart, A. (2008). Multiscale methods: averaging and homogenization. Springer Science & Business Media.
[30] Da Prato, G., & Zabczyk, J. (2014). Stochastic equations in infinite dimensions. Cambridge university press.
[31] Prévôt, C., & Röckner, M. (2007). A concise course on stochastic partial differential equations. Berlin, Heidelberg: Springer Berlin Heidelberg.
[32] Blömker, D., Hairer, M., & Pavliotis, G. A. (2007). Multiscale analysis for stochastic partial differential equations with quadratic nonlinearities. Nonlinearity, 20(7), 1721-1744.
[33] Roberts, A. J. (2008). Normal form transforms separate slow and fast modes in stochastic dynamical systems. Physica A: Statistical Mechanics and its Applications, 387(1), 12-38.
[34] Blömker, D., & Mohammed, W. W. (2013). Amplitude equations for SPDEs with cubic nonlinearities. Stochastics An International Journal of Probability and Stochastic Processes, 85(2), 181-215.
[35] Mohammed, W. W., Blömker, D., & Klepel, K. (2014). Multi-scale analysis of SPDEs with degenerate additive noise. Journal of Evolution Equations, 14(2), 273-298.
[36] Galvele, J. R. (1976). Transport processes and the mechanism of pitting of metals. Journal of the Electrochemical Society, 123(4), 464-474.
[37] Caffarelli, L., & Silvestre, L. (2007). An extension problem related to the fractional Laplacian. Communications in partial differential equations, 32(8), 1245-1260.
[38] Di Nezza, E., Palatucci, G., & Valdinoci, E. (2012). Hitchhiker's guide to the fractional Sobolev spaces. Bulletin des sciences mathématiques, 136(5), 521-573.
[39] Henry, D. (2006). Geometric theory of semilinear parabolic equations. Springer.
[40] Temam, R. (2012). Infinite-dimensional dynamical systems in mechanics and physics. Springer Science & Business Media.
[41] Allman, E. S., & Rhodes, J. A. (2004). Mathematical models in biology: an introduction. Cambridge University Press.
[42] Smoller, J. (2012). Shock waves and reaction—diffusion equations (Vol. 258). Springer Science & Business Media.
[43] Glass, G. K., & Buenfeld, N. R. (2000). The influence of chloride binding on the chloride induced corrosion risk in reinforced concrete. Corrosion Science, 42(2), 329-344.
[44] Ann, K. Y., & Song, H. W. (2007). Chloride threshold level for corrosion of steel in concrete. Corrosion science, 49(11), 4113-4133.
[45] Meerschaert, M. M., & Sikorskii, A. (2019). Stochastic models for fractional calculus (Vol. 43). Walter de Gruyter GmbH & Co KG.